Single molecule studies reveal temperature independence of lifetime of dynamic heterogeneity in polystyrene

Alyssa S. Manz,[1] Keewook Paeng,[1,2] and Laura J. Kaufman[1,a)]
[1]*Department of Chemistry, Columbia University, New York, New York 10027, USA*
[2]*Department of Chemistry, Sungkyunkwan University, Suwon 16419, South Korea*

(Received 28 March 2018; accepted 10 May 2018; published online 29 May 2018)

Polymeric systems close to their glass transition temperature are known to exhibit heterogeneous dynamics that evolve both over time and space, comparable to the dynamics of small molecule glass formers. It remains unclear how temperature influences the degree of heterogeneous dynamics in such systems. In the following report, a fluorescent perylene dicarboximide probe molecule that reflects the full breadth of heterogeneity of the host was used to examine the temperature dependence of the dynamic heterogeneity lifetime in polystyrene at several temperatures ranging from the glass transition to 10 K above this temperature via single molecule microscopy. Contrary to prior reports, no apparent temperature dependence of time scales associated with dynamic heterogeneity was detected; indeed, the probe molecules report characteristic dynamic heterogeneity lifetimes 100–300 times the average alpha-relaxation time (τ_α) of the polystyrene host at all temperatures studied. *Published by AIP Publishing.* https://doi.org/10.1063/1.5031131

INTRODUCTION

The study of fundamental properties of polymeric systems near their glass transition temperatures (T_g) has been an active area of research for decades. In part due to the ubiquity of thin polymeric films in emerging technologies, including in organic optoelectronics, coatings, and battery cells, there has been heightened focus on the properties and surface molecular dynamics of such films.[1–3] However, even aspects of the properties of bulk polymeric films are poorly understood owing to the incomplete understanding of the glass transition and molecular motion as it occurs in systems near their glass transition temperatures.[4]

Both amorphous polymers and small molecule liquids near their glass transition temperatures display non-exponential fluctuations and relaxations, which have been characterized using a variety of techniques. Such non-exponential behaviors have been associated with dynamic heterogeneity, in which dynamics vary both as a function of position (spatial heterogeneity) and over time (temporal heterogeneity) even in the absence of identifiable structural heterogeneity.[5,6] The causal relationship between the emergence of dynamic heterogeneity and the extreme slowdown of dynamics in liquids as they approach the glass transition is not entirely clear. However, the observation that dynamic heterogeneity in the absence of structural heterogeneity occurs always and only alongside an approaching glass transition encourages continued study and characterization of the spatial and temporal character of dynamic heterogeneity. Simulations and a few experiments have suggested that relevant length scales of heterogeneity are just a few nanometers, making them very difficult to directly access experimentally.[7–11]

Time scales associated with dynamic heterogeneity are much more accessible in typical experiments, and thus persistence of dynamic heterogeneity has been studied quite extensively, typically characterized through an exchange time (τ_{ex}) or a dynamic heterogeneity lifetime (τ_{hetero}). While various definitions exist, we will distinguish exchange time and dynamic heterogeneity lifetime as follows: τ_{ex} describes the time a particular molecule displays dynamics characterized by a well-defined time scale before transitioning to a different well-defined time scale, while τ_{hetero} refers to the time over which a molecule or set of molecules exhibits particular dynamics that are distinct from those of other sub-ensembles in the system. Substantial differences in exchange time and dynamic heterogeneity lifetime have been reported across systems and techniques, with some differences attributed to the fact that measurements have been performed at different temperatures relative to T_g, and these quantities may vary with temperature, though no consensus currently exists on their temperature dependence.[5,12–23]

Over the past decade, single molecule experiments have been used to characterize aspects of dynamic heterogeneity in polymeric systems.[23–30] Recently, we used single molecule measurements of rotational motion of probe molecules in polystyrene to characterize the range of exchange times present in this system. This study, performed at the single temperature of ≈378 K (T_g + 5 K; 1.01 T_g), revealed that exchange between environments with distinct dynamics occurs over a broad range of time scales, including those as short as 70 τ_α, with τ_α being the alpha-relaxation time in polystyrene, which corresponds to the segmental dynamics of the host polymer. Our study revealed several characteristic time scales associated with dynamic exchange, including ≈2300 τ_α as the time in which the average molecule explored most environments in the system and ≈35 000 τ_α as the extrapolated time at which every molecule would have explored all

a)Author to whom correspondence should be addressed: kaufman@chem.columbia.edu

environments in the system. To obtain closer analogy to measurements that have characterized the lifetime of dynamic heterogeneity in glassy systems through sub-ensemble approaches, we also stratified molecules into fast and slow sub-ensembles and found that initially fast molecules randomize on a time scale of ≈60 τ_α and slow ones on a time scale of ≈250 τ_α. These time scales are somewhat longer than those measured previously in polystyrene at some temperatures; however, a prior experiment has shown strong temperature dependence of the lifetime of dynamic heterogeneity in PS in the range of T_g–T_g + 10 K.[15] Here, we aim to resolve outstanding questions regarding the temperature dependence of the lifetime of dynamic heterogeneity in polystyrene near T_g through single molecule measurements and a variety of data analysis approaches.

MATERIALS AND METHODS

Sample preparation

Polystyrene (M_w = 168 kg/mol, PDI = 1.05) was obtained from Polymer Source, re-precipitated in hexane three times, and then dissolved in toluene. The 3.4 wt. % polystyrene in toluene solution was photobleached in a home-built, high power light emitting diode based setup for at least 48 h to achieve a non-fluorescent host. Silicon wafers were cut into 6.5 × 6.5 mm pieces and cleaned with piranha solution (H_2SO_4:H_2O_2 = 1:1). The fluorescent dye *N*,*N*′-dipentyl-3,4,9,10-perylenedicarboximide (pPDI) was obtained from Sigma-Aldrich and diluted to 5 × 10^{-9}M. 4 μl was then added to 400 μl of the polystyrene solution, resulting in a solution of ≈5 × 10^{-11}M. The solution was then spin-coated at 2000 rpm onto a cleaned silicon wafer, which resulted in a film of ≈200 nm thickness as measured by ellipsometry. We note that the films were sufficiently thick such that bulk dynamics dominated. Molecules in near vicinity of the supported and free surfaces are unlikely to be detected in our study due to a combination of their relative rarity in the sample, potential quenching near the silicon surface, and the dynamic range of the measurement, which is 1–2 orders of magnitude in detected relaxation times for a given frame rate, as chosen for each temperature interrogated.[1,23,24,31,32] After spin-coating, the final fluorophore concentration was ≈2 × 10^{-9}M, sufficiently dilute to avoid multiple probe molecules within a diffraction limited spot yet concentrated enough to provide on average 200 analyzable fluorophores per field of view.

The sample was placed in a vacuum cryostat (Janis ST-500) integrated with a home-built wide-field microscope. The cryostat provides temperature control, facilitates removal of toluene from the sample, and limits oxygen-induced photobleaching of the fluorescent probes. Once the sample was placed in the cryostat, the pressure was lowered to ≈1.8 mTorr and the temperature was raised to a minimum of 10 K above the glass transition temperature (383–385 K) and held there for at least 1 h to assist in removal of the residual solvent and ensure stable pressure.[1] Given that the temperatures probed were so close to the glass transition temperature, the sample was then lowered to the measurement temperature and held there for an additional 2–3 h to ensure the system was at equilibrium and not an aging glass. This was confirmed by the temperature-dependence of the rotational relaxation time, τ_c, as shown in Fig. 1.

Imaging

A continuous wave diode Nd:Vanadate laser (532 nm) was coupled into a multimode fiber, which was shaken at constant frequency and amplitude by a speaker to eliminate speckles and produce a randomly polarized and homogeneously illuminated field of view (diameter ≈100 μm). The light was then focused at the back of the objective lens [Zeiss, LD Plan-Neofluar, air 63×, NA = 0.75] and into the cryostat to illuminate the sample. Fluorescence was collected in the epi-direction, through the same objective lens, and then passed through a dichroic mirror, a long-pass (Semrock, LP03-532RU-25), and a bandpass filter (Semrock, FF01-582/75). A Wollaston prism was used to split the image into orthogonal polarizations, which were imaged onto an electron multiplying charge-coupled device camera (EMCCD; Andor iXon DV887). Excitation power was 15 mW at the back of the objective lens, corresponding to a power density of 150 W/cm^2 at the sample. Frame rate was chosen to be ≈20 frames per median relaxation time (τ_{fit}) for the longest movies and was 0.143 Hz (373.0 K), 5.0 Hz (378.1 K), 14.8 Hz (379.6 K), and 124.8 Hz (383.6 K). For movies collected at the highest temperature, only a portion of the CCD chip was used to maximize the frame rate. Movies with a frame rate >5 Hz were collected continuously while slower frame rate movies were collected with a 0.2 s exposure time, with illumination shuttered between frames to limit photobleaching. For each temperature, several long movies were collected on the same sample, such that data were collected from at least 1000 molecules at each temperature. Portions of representative movies at each temperature are shown in Videos S1–S4 of the supplementary material. We corrected from set temperatures to measured temperatures to account for a small degree of sample heating using power dependence measurements in *o*-terphenyl (OTP),[33] and all temperatures reported are corrected temperatures. In both *o*-terphenyl and polystyrene, sample heating is expected to result solely from substrate heating as the hosts do not absorb at 532 nm. Hence, the temperature increase as a function of excitation power is expected to be host independent.

Data analysis

Single molecule linear dichroism imaging[34] and analysis for the purposes of evaluating heterogeneous dynamics have been described previously.[35–37] For this work, all analysis was performed using Interactive Data Language (IDL) software (ITT Visual Information Solutions), as described in detail in the studies of Hoang *et al.* and Mackowiak *et al.*[6,37] Due to the slow rotations and thus long duration of data acquisition at the lowest temperature, movies at 373.0 K were de-drifted prior to analysis. For data collected at all temperatures, molecules were chosen from a bandpassed set of 500 summed images, found in the temporal middle of the longest movies, using the "feature" algorithm as described by Crocker and Grier.[38] Subsequent analysis was performed on

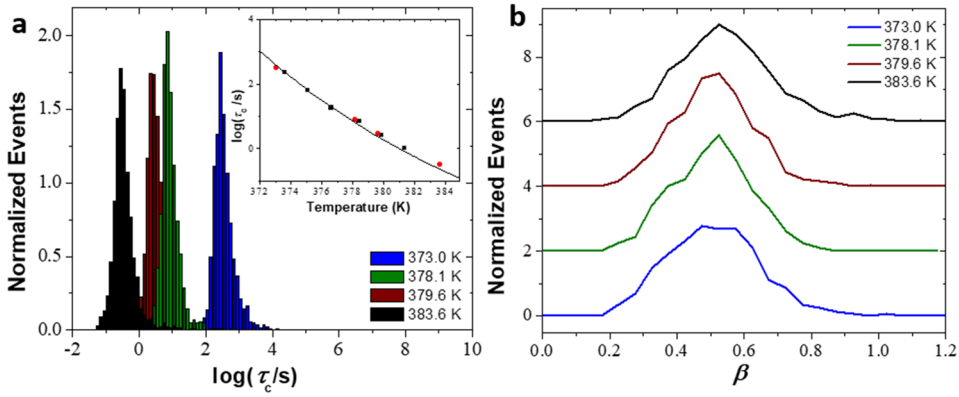

FIG. 1. (a) Normalized distributions of τ_c at the longest trajectory studied over the temperature range $T_g - T_g + 10$ K ($T_g - 1.03\ T_g$), with the inset showing median τ_c values at each temperature probed (red circles). The data are compared to previously published values (black squares) by Paeng *et al.*, with the line drawn being the VFT fit to the temperature dependence as reported by Roland and co-workers from dielectric spectroscopy measurements and shifted by 0.85 decades.[41,42] (b) Vertically offset normalized distributions of β values at each temperature. Detailed characteristics of the data sets and distributions are given in Table S1 of the supplementary material.

the raw and unfiltered images. Polarized fluorescence intensities (I_s, I_p) of the selected molecules were extracted from the two orthogonal polarization images of each molecule collected on the CCD at each time point. Single molecule linear dichroism (LD) was then calculated via $LD(t) = (I_s - I_p)/(I_s + I_p)$, of which an autocorrelation function (ACF) was constructed using $[\sum_{t'} a(t') \cdot a(t'+t)]/[\sum_{t'} a(t') \cdot a(t')]$, where $a(t) = LD(t) - \langle LD(t) \rangle$. Least-squares fitting was used to fit each autocorrelation function (ACF) to a stretched exponential function, $C(t) = C(0) \cdot \exp[-(t/\tau_{fit})^{\beta}]$. For the analysis of full-length movies, the correlation function was fit until it decayed to 0.1. C(t) values were constrained to $0.2 < \beta < 2.0$ and $0.3 < C(0) < 2.0$, and the average rotational correlation time, τ_c, was calculated from the fit values of τ_{fit} and β via $\tau_c = (\tau_{fit}/\beta) \cdot \Gamma(1/\beta)$, where Γ is the gamma function. Following analysis of the full-length movies, movies were cut to a specified number of frames to allow analysis of single molecule dynamics as a function of trajectory length. For some analyses (as described in the section titled Results), the same molecules that were analyzed in the longest movies were also selected in the cut movies for data analysis while in other analyses all analyzable molecules were retained regardless of whether they were analyzed in the full length movies. For analyses in which tracking specific molecules as a function of trajectory length was performed, initial feature finding was performed from the shortest trajectory length data. For such analysis, the constraints for β and C(0) were lifted and the only constraint applied was (number of frames)/$\tau_{fit} \geq 2$.

Simulations

Simulations of homogeneous rotational diffusion were carried out as previously described so that effects of finite trajectory length on measured τ_{fit} and β values (independent of dynamic heterogeneity) could be assessed.[39] Briefly, probes were set to have a diffusion constant, D_r, by rotating a unit vector ϕ through an angle chosen from a Rayleigh distribution of width $\sqrt{2D_r}$. The rank-l rotational autocorrelation function is given by $C_l(t) = \langle P_l(\hat{\phi}(t_0) \cdot \hat{\phi}(t_0 + t)) \rangle_{t_0}$, where $P_l(x)$ is the rank-l Legendre polynomial and the average is performed over the trajectory. For isotropic probes undergoing homogeneous rotational diffusion through small angular displacements, all ranks exhibit exponential relaxation, $C_l(t) = e^{-l(l+1)D_r t} \equiv e^{-t/\tau_l}$, where $\tau_l \equiv (l(l+1)D_r)^{-1}$ is the relaxation time scale of the local environment. The second rank autocorrelation function strongly dominates linear dichroism measurements, thus for the data presented in this study $\tau_r \equiv \tau_2$.[40] The diffusion constant was chosen such that $\tau_r = 100$ steps and each trajectory length simulated consisted of 500 molecules. For each simulated probe, an autocorrelation was computed and fit to a stretched exponential and all data analysis was performed as for experimental data.

RESULTS

In advance of using pPDI as a probe with which to interrogate the temperature dependence of the lifetime of dynamic heterogeneity in polystyrene, we first confirmed that pPDI acts as an ideal single molecule probe for polystyrene. To demonstrate a single molecule probe is an ideal probe for a given host requires demonstrating that the probe dynamics are slaved to those of the host and that the probes report the full extent of heterogeneity in the system, as characterized in bulk probe-free experiments. Both results were shown previously for pPDI in polystyrene, though here we cover a broader temperature range than in the previous work.[41] Briefly, each single molecule linear dichroism auto-correlation constructed from trajectories of given length was fit to the Kohlrausch-Williams-Watt equation, $C(t) = C(0) \exp[-(t/\tau_{fit})^{\beta}]$, and τ_{fit}, β, and τ_c were obtained from each single molecule trajectory as described in the section titled Materials and Methods.

Distributions of τ_c at temperatures between 373.0 and 383.6 K for trajectories of ≈900 τ_{fit} in length at each temperature are shown in Fig. 1(a). As in the previous report, distributions are approximately log-normal and show no notable shape difference as a function of temperature. Median τ_c values are shown in Fig. 1(a), inset, and fit to a Vogel-Fulcher-Tannmann (VFT) curve, consistent with previous single molecule and bulk measurements in polystyrene, which demonstrates that probe molecules follow the dynamics of the host.[41,42] While the temperature dependence of the probe rotation tracks that

of the host segmental dynamics, the probe rotational correlation time is ≈0.85 decades or ≈7 times slower than the host segmental dynamics (τ_c/τ_α = 7.07). Given the fact that the probe rotates slower than the host segmental dynamics, it is possible that the probe averages over some dynamic heterogeneity in the system. To ensure pPDI accesses and can report the full breadth of dynamic heterogeneity as reflected by bulk probe-free experiments, the median stretching exponent was examined. Distributions of stretching exponents, β, obtained from the same data from which τ_c values were obtained are plotted in Fig. 1(b). Median β values are ≈0.5 and do not vary as a function of temperature, consistent with previous bulk measurements.[43] While there are various literature values of probe-free or small probe ensemble or sub-ensemble measurements of β in moderate molecular weight polystyrene near T_g, most are similar to the median values obtained in this study.[15,42–44] The data in Fig. 1 verify that pPDI reflects the dynamic heterogeneity of the host. Moreover, it adds additional evidence that for trajectories of a given length, single molecule reports return distributions of τ_c and β values that do not vary as a function of temperature near T_g, with the current study providing the largest temperature range probed with an ideal probe to date.[31,41]

In previous work, pPDI dynamics in PS were evaluated as a function of trajectory length, which is equivalent to observation time, to identify time scales associated with temporal heterogeneity in the system at T_g + 5 K. Here we present the first ideal probe measurements of the lifetime of dynamic heterogeneity across temperatures. First, data were collected for trajectory lengths of ≈900 τ_{fit} at each of four temperatures, with the data shown in Fig. 1 obtained from these long trajectories. At all temperatures, single molecule trajectories were then truncated to a variety of lengths from ≈18 to 500 τ_{fit}, autocorrelations were re-constructed and re-fit, and τ_{fit} and β distributions were obtained. The distributions associated with measurements of the lowest and highest temperatures interrogated, 373.0 K and 383.6 K, are shown in Figs. 2(a)–2(d) as a function of trajectory length. At both temperatures, as well as at the other two temperatures at which data were collected, with increasing observation time the τ_{fit} and β distributions get narrower and the median β value shifts from near 1.0 to near 0.5, indicative of molecules sampling different dynamic environments as the observation window increases. To further quantify how these distributions change as a function of trajectory length and temperature, the distribution width (FWHM) and, in the case of β, median value, were assessed for all temperatures investigated as a function of trajectory length [Figs. 2(e) and 2(f)]. This reveals that at all temperatures studied, τ_{fit} and β distributions evolve in a very similar manner. The smooth evolution of β_{med} from ≈1 at the shortest trajectory evaluated (≈20τ_{fit}) to that associated with a bulk measurement at the longest trajectories evaluated (≈900τ_{fit}) confirms that dynamic exchange occurs over that range of time scales for all temperatures interrogated.

To characterize the lifetime of dynamic heterogeneity in polystyrene more precisely, for data collected at each temperature, molecules analyzed were grouped into five sub-ensembles based on their initial τ_{fit} values. For each movie, molecules were characterized at the ≈18 τ_{fit} trajectory length, and the same molecules were analyzed at trajectories of

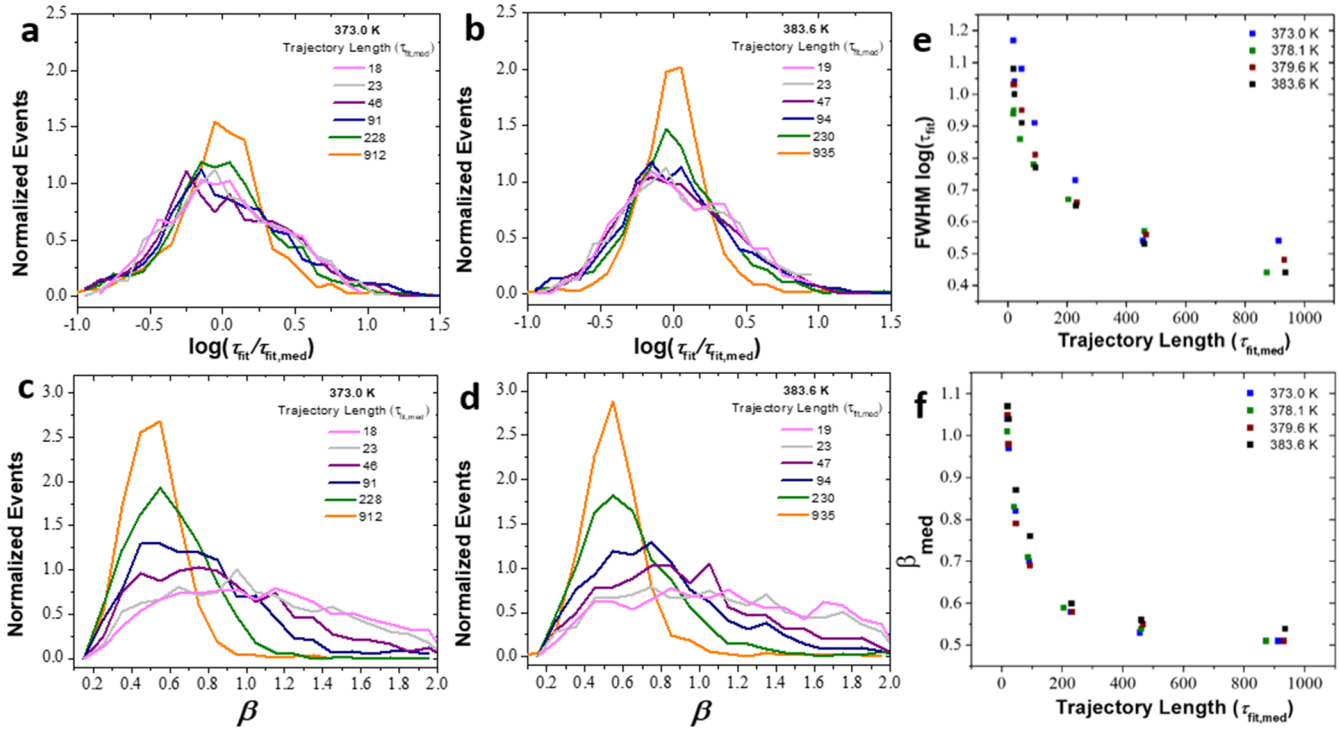

FIG. 2. Rotational relaxation measurements as a function of trajectory length for the lowest and highest temperatures probed. Normalized τ_{fit} distribution at all trajectory lengths at (a) 373.0 K and (b) 383.6 K and β distributions at (c) 373.0 K and (d) 383.6 K. The evolution of (e) the FWHM of log(τ_{fit}) and (f) median β with trajectory length from the distributions shown in (a)–(d) as well as equivalent data at the other temperatures studied. Detailed characteristics of the data sets and distributions are given in Table S2 of the supplementary material.

≈23, 45, 90, 225, and 900 τ_{fit}. The τ_{fit} values for each molecule at the 18 τ_{fit} trajectory were used to determine sub-ensembles, and three sub-ensembles (the fastest fifth of molecules, slowest fifth of molecules, and the fifth of molecules in the center of the τ_{fit} distribution) were analyzed for their dynamical evolution as a function of trajectory length or observation time. We note that this analysis is distinct from that described above and depicted in Fig. 2, as here particular molecules are tracked as a function of observation time while in the previous analysis all molecules were included. This analysis, therefore, clarifies how long molecules that are, for example, slow upon initial (short) observation window, remain among the slowest in the distribution as a function of observation time. Figure 3(a) reveals that all temperatures studied show the same trend: initially, the fastest and slowest molecules are clearly separated, with τ_{fit} values differing by approximately a factor of 10. As observation time increases, the initially fastest and slowest molecules converge. We note that in all cases, the central sub-ensemble, representing average molecules, slows to a certain extent as observation time increases. This points to the limited dynamic range of measurements as short as 18 τ_{fit}, which cannot fully capture the dynamics of the slowest sub-set of molecules.

To assess whether statistical effects associated with analysis of short trajectories play a role in the measured spread between the fastest and slowest sub-ensembles, particularly for short trajectories, simulations of probes exhibiting homogeneous dynamics (with τ_{fit} = 100s) were analyzed in the same manner as experimental results. These simulations show limited spread in τ_{fit} dynamics but a large spread, comparable to that seen experimentally, in τ_c dynamics (Fig. S1 of the supplementary material). This large spread in the simulated τ_c data arises from the strong effect of short trajectories on measured β values and points to the importance of evaluating experimental τ_{fit} rather than τ_c data for such analysis.[39,45,46] Comparing the simulated and experimental τ_{fit} data confirms that the spread seen in the experimental results is not due to statistical effects associated with analysis of short trajectories. Instead, the convergence in dynamics of the initially fastest and slowest molecules requires that the probes experience distinct dynamics, through dynamical evolution of the local environment over time and/or through the probe physically moving from a region of given dynamics to a region of distinct dynamics. Importantly, the time over which the sub-ensembles converge occurs at approximately the same trajectory length, or observation time, in terms of τ_{fit} for all temperatures [Fig. 3(a)]. This time to convergence can be considered the lifetime of dynamic heterogeneity, τ_{hetero}, as it marks the time required for initially distinct dynamic sub-ensembles to become indistinguishable.

To quantitatively characterize the time scale over which the sub-ensembles converge as a function of observation time, the difference in median log(τ_{fit}) of the fastest and slowest subsets of molecules was analyzed [Fig. 3(b)]. At first, a large difference between sub-ensembles is observed, with Δ[log(τ_{fit})] ≈ 1 for all temperatures, indicating that the molecules' rotational correlation times span approximately one decade at short times, consistent with the data presented in Fig. 2 and Table S2 of the supplementary material. As observation time increases, Δ[log(τ_{fit})] values decrease and reach ≈0 at the longest trajectory lengths. This demonstrates that molecules that started out both particularly fast and particularly slow have sufficiently sampled the range of dynamic environments in the system to report the same average relaxation time at long observation times. To quantify the lifetime of dynamic heterogeneity, the evolution of the Δ[log(τ_{fit})] values shown in Fig. 3(b) were fit to exponential decays (Fig. S2 of the supplementary material). At all temperatures, the characteristic time required for molecules in the slow and fast sub-ensembles to converge was between 40 and 80 τ_{fit} (140–280 τ_α), with no trend as a function of temperature. To quantitatively compare the evolution of the full distribution (Fig. 2) to that associated with molecules from particular sub-ensembles [Figs. 3(a) and 3(b)], we looked at the difference between the median fastest and slowest portions of the distribution without following individual molecules. This difference converges more slowly than the rotational correlation times of tracked molecules [Fig. 3(c)], indicating that there is no tendency for molecules in a particular dynamic sub-ensemble at the beginning of the experiment to stay in that dynamic sub-ensemble, and indeed the fastest molecules may become among the slowest and vice-versa over time.

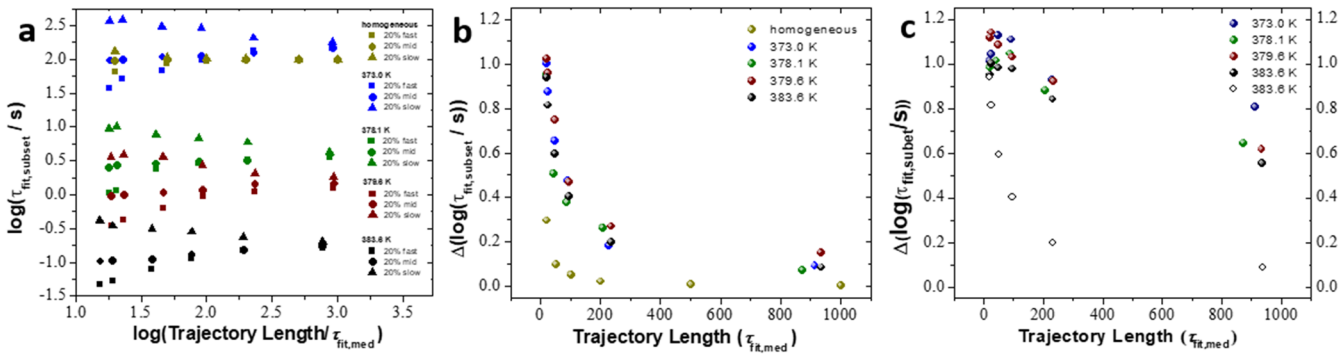

FIG. 3. (a) Median τ_{fit} values as a function of trajectory length for the 20% initially fastest (squares), initially slowest (triangles), and initially average (circles) molecule sub-ensembles at each temperature studied, as well as for a homogeneous simulation. (b) Difference between the median log(τ_{fit}) values of the initially slowest and fastest molecules at each temperature as well as for a homogeneous simulation. (c) (solid symbols) Δ[log($\tau_{fit,subset}$)] of the 20% slowest and 20% fastest molecules at all trajectory lengths without following individual molecules and (open symbols) Δ[log($\tau_{fit,subset}$)] at 383.6 K, also shown in Fig. 3(b).

DISCUSSION

Using single molecule fluorescence microscopy, rotational dynamics in polystyrene at temperatures from T_g to $T_g + 10$ K were studied. The lifetime of dynamic heterogeneity showed no trend as a function of temperature when considering either (1) how the full distributions of rotational relaxation times and stretching exponents evolved as a function of observation time (Fig. 2) or (2) how molecules initially in particular dynamic sub-ensembles evolved toward the average (Fig. 3). From the latter analysis, designed to mimic aspects of earlier sub-ensemble NMR and photobleaching experiments,[14,15,47] the average lifetime of dynamic heterogeneity was found to be $\approx 60\ \tau_{fit}$ ($\approx 210\ \tau_\alpha$), with fast and slow initial sub-ensembles fully randomizing on this time scale at all temperatures probed.

The dynamic heterogeneity and its temperature independence relative to τ_α is in partial contradiction to several previous studies that have shown a temperature dependence for exchange time.[14,15] Differences in the host matrix, temperatures probed, dynamic range of the experiments, sub-ensemble considered, and dynamic heterogeneity lifetime definitions may explain at least a subset of differences that have been observed. For example, simulations have shown that dynamic heterogeneity lifetime is system dependent, with more fragile systems exhibiting both longer lived dynamic heterogeneities at a given temperature and stronger temperature dependence of the dynamic heterogeneity lifetime.[48,49] Indeed, in a recent study, the lifetime of dynamic heterogeneity, τ_{hetero}, for an array of model supercooled systems was obtained from relaxation of a three-time correlation function and was found to vary as $\tau_{hetero} \sim \tau_\alpha^{0.9} - \tau_\alpha^{1.9}$.[49] Our measurement yields a result in this range, with $\tau_{hetero} \sim \tau_\alpha$, with τ_{hetero} defined by the convergence of the fast and slow sub-ensembles through fits to the data presented in Fig. 3(b) (Fig. S2 of the supplementary material).

Experimentally, the temperature dependence of the lifetime of dynamic heterogeneity was addressed by Ediger and co-workers in supercooled *o*-terphenyl (OTP) following two earlier reports, each of which characterized the quantity at a single temperature.[14,47,50] Initially, Cicerone and Ediger used a photo-bleaching technique to probe a sub-ensemble of slow probe molecules in OTP at $T_g + 1$ K while Böhmer and co-workers used multi-dimensional NMR to interrogate slow sub-ensembles of neat OTP at $T_g + 10$ K.[47,50] These studies, together with a follow-up study by Ediger and co-workers, suggested that the dynamic heterogeneity lifetime was strongly temperature dependent in this system, with τ_{hetero} increasing relative to τ_α as temperature decreased.[14] A later study using the same techniques in polystyrene yielded similar results: here, photobleaching measurements revealed that dynamic heterogeneity varied from $\approx 11\ \tau_\alpha$ at $T_g + 2$ K to $65\ \tau_\alpha$ at T_g for the smallest probe employed.[15] In this study, a deep photobleach was used to preferentially bleach molecules that were rotating quickly relative to the average molecule, leaving behind a slow sub-ensemble that was interrogated after variable waiting time. While the analysis performed in Fig. 3 in some ways approximates this approach, a more directly analogous analysis can be achieved starting with single molecule trajectories. Here, a fast and slow subset of molecules are followed, but in contrast to the analysis shown in Fig. 3, dynamics are not averaged over increasing observation windows and instead are assessed for a given amount of time ($100\ \tau_{fit}$) as a function of increasing waiting time between two such windows (Fig. 4). Unlike the other approaches used here as well as a window-sliding approach used previously,[23,33,37] this approach provides a history independent accounting of dynamic heterogeneity lifetime. Again, no temperature dependence of the extracted dynamic heterogeneity lifetimes is seen, consistent with all other approaches we used to characterize dynamic heterogeneity lifetime.

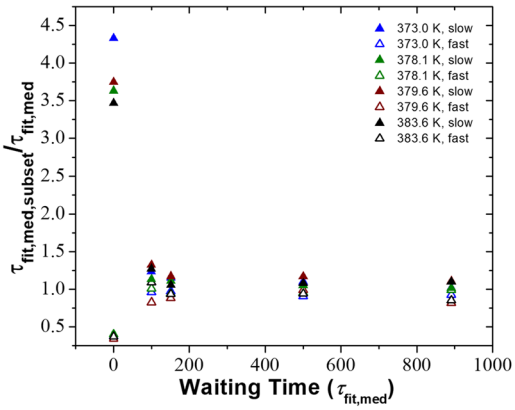

FIG. 4. Median τ_{fit} for fast (open symbols) and slow (closed) subsets relative to the median τ_{fit} for all molecules as a function of waiting time between $100\ \tau_{fit}$ trajectory length assessed windows. Sub-ensembles were determined from the initial $100\ \tau_{fit}$ window (waiting time = 0) and subsequent $\tau_{fit,med,subset}$ values were obtained from the same molecules interrogated during a second $100\ \tau_{fit}$ window a waiting time later.

To quantify dynamic heterogeneity lifetime using this approach, the data in Fig. 4 were fit to exponential decays and a characteristic time scale was extracted (Fig. S3 of the supplementary material). For the slow subset of molecules, we find dynamic heterogeneity lifetimes of 30–40 τ_{fit} (105–140 τ_α) with no trend as a function of temperature. The fast subset evolves more quickly such that nearly all relaxation time randomization occurs within the first waiting time window, preventing extraction of dynamic heterogeneity lifetimes for this fast subset of molecules. We note that while the temperature (in)dependence is clearly distinct in our measurements relative to previous measurements, the absolute values of the lifetime of dynamic heterogeneity in polystyrene are more similar to those reported previously once single molecule data analysis proceeds in a manner more closely approximating the earlier experimental approach.

The lack of temperature dependence of the dynamic heterogeneity lifetime is not the only difference in this experiment compared to that of Ediger and co-workers.[15] Notably, the slow sub-ensemble in the current experiment is 3.5–4.5 times slower than the median at each temperature while the slow sub-ensemble in Ref. 15 was a factor of 1.1–2.0 (with some temperature and probe variation) slower than average, suggesting that our sub-ensemble is distinct from that studied by Ediger *et al.*, which could account for differences between our and their findings on the temperature dependence of τ_{hetero} relative to τ_α.

Our findings of temperature independence of τ_{hetero} ($\tau_{hetero} \sim \tau_\alpha$) are consistent with the fact that for long trajectory lengths,

we find no difference in the median single molecule β value or distribution of β, τ_{fit}, or τ_c values as a function of temperature, each of which suggests there is no difference in degree of dynamic heterogeneity in polystyrene over the temperature range investigated. The behavior of the stretching exponent β for a system over a given temperature range appears to be a strong predictor of the temperature dependence of the lifetime of dynamic heterogeneity, with those systems with limited β change over temperature also showing limited or no change in dynamic heterogeneity lifetime relative to structural relaxation time with temperature.[48,49,51,52] The scaling of τ_{hetero} with τ_α in polystyrene over the approximately three orders of magnitude variation in alpha-relaxation explored here leaves open the possibility that the segmental relaxation of the polymer and the randomization of distinct dynamic environments across the system are governed by a single process. This finding also suggests limited growth in domains of slow dynamics and locally preferred structures in polystyrene with cooling over the range of relaxation time scales interrogated;[49] this behavior may prove to be a distinction between polymers, which tend to have relatively weak β dependence on temperature,[53] and small molecule supercooled liquids, though experimental approaches to directly identifying such structures in polymeric and molecular systems are currently lacking.

CONCLUSIONS

We investigated the temperature dependence of the dynamic heterogeneity lifetime in polystyrene near its glass transition temperature using a single molecule approach in which the rotations of an ideal probe, pPDI, reported the dynamics and dynamic heterogeneity of the host polystyrene over the temperature range of $T_g - T_g + 10$ K. Applying various data analysis approaches, no temperature dependence of the lifetime of dynamic heterogeneity relative to τ_α in the studied temperature range was detected. By following sub-ensembles of fast and slow molecules as their dynamics evolve toward that of the average molecule as a function of observation time, we identified a characteristic lifetime of dynamic heterogeneity between 140 and 280 τ_α with no apparent trend as a function of temperature.

SUPPLEMENTARY MATERIAL

See supplementary material for two tables associated with data in Fig. 1 and Fig. 2, three figures [Figs. 3(b) and 4 with fits and a τ_c analog of Fig. 3(a)], and four representative videos.

ACKNOWLEDGMENTS

This work was supported by the National Science Foundation under Grant Nos. DGE 16-44869, CHE 1213242, and CHE 1660392.

[1] K. Paeng, S. F. Swallen, and M. D. Ediger, J. Am. Chem. Soc. **133**, 8444 (2011).
[2] Z. Fakhraai and J. A. Forrest, Science **319**, 600 (2008).
[3] M. D. Ediger and J. A. Forrest, Macromolecules **47**, 471 (2014).
[4] K. L. Ngai, J. Non-Cryst. Solids **275**, 7 (2000).
[5] L. A. Deschenes and D. A. Vanden Bout, J. Phys. Chem. B **106**, 11438 (2002).
[6] D. Hoang, K. Paeng, H. Park, L. Leone, and L. J. Kaufman, Anal. Chem. **86**, 9322 (2014).
[7] U. Tracht, M. Wilhelm, A. Heuer, H. Feng, K. Schmidt-Rohr, and H. W. Spiess, Phys. Rev. Lett. **81**, 2727 (1998).
[8] C. Donati, S. C. Glotzer, and P. H. Poole, Phys. Rev. Lett. **82**, 5064 (1999).
[9] S. A. Reinsberg, X. H. Qiu, M. Wilhelm, H. W. Spiess, and M. D. Ediger, J. Chem. Phys. **114**, 7299 (2001).
[10] N. Lačević, F. W. Starr, T. B. Schroder, and S. C. Glotzer, J. Chem. Phys. **119**, 7372 (2003).
[11] B. Rijal, L. Delbreilh, and A. Saiter, Macromolecules **48**, 8219 (2015).
[12] A. Heuer and K. Okun, J. Chem. Phys. **106**, 6176 (1997).
[13] J. Qian and A. Heuer, Eur. Phys. J. B **18**, 501 (2000).
[14] C. Wang and M. D. Ediger, J. Phys. Chem. B **103**, 4177 (1999).
[15] C. Y. Wang and M. D. Ediger, J. Chem. Phys. **112**, 6933 (2000).
[16] A. N. Adhikari, N. A. Capurso, and D. Bingemann, J. Chem. Phys. **127**, 114508 (2007).
[17] U. Pschorn, E. Rossler, H. Sillescu, S. Kaufmann, D. Schaefer, and H. W. Spiess, Macromolecules **24**, 398 (1991).
[18] H. Mizuno and R. Yamamoto, Phys. Rev. E **82**, 030501 (2010).
[19] H. Mizuno and R. Yamamoto, Phys. Rev. E **84**, 011506 (2011).
[20] R. Böhmer, G. Diezemann, G. Hinze, and H. Sillescu, J. Chem. Phys. **108**, 890 (1998).
[21] K. Kim and S. Saito, J. Chem. Phys. **133**, 044511 (2010).
[22] K. Kim and S. Saito, J. Non-Cryst. Solids **357**, 371 (2011).
[23] A. Schob, F. Cichos, J. Schuster, and C. von Borczyskowski, Eur. Polym. J. **40**, 1019 (2004).
[24] B. M. I. Flier, M. C. Baier, J. Huber, K. Müllen, S. Mecking, A. Zumbusch, and D. Wöll, J. Am. Chem. Soc. **134**, 480 (2012).
[25] A. Deres, G. A. Floudas, K. Müllen, M. Van der Auweraer, F. De Schryver, J. Enderlein, H. Uji-i, and J. Hofkens, Macromolecules **44**, 9703 (2011).
[26] H. Uji-i, S. M. Melnikov, A. Deres, G. Bergamini, F. De Schryver, A. Herrmann, K. Müllen, J. Enderlein, and J. Hofkens, Polymer **47**, 2511 (2006).
[27] S. Adhikari, M. Selmke, and F. Cichos, Phys. Chem. Chem. Phys. **13**, 1849 (2011).
[28] C.-Y. J. Wei and D. A. Vanden Bout, J. Phys. Chem. B **113**, 2253 (2009).
[29] B. M. I. Flier, M. Baier, J. Huber, K. Müllen, S. Mecking, A. Zumbusch, and D. Wöll, Phys. Chem. Chem. Phys. **13**, 1770 (2011).
[30] G. Hinze, T. Basché, and R. A. L. Vallée, Phys. Chem. Chem. Phys. **13**, 1813 (2011).
[31] K. Paeng, H. Park, D. T. Hoang, and L. J. Kaufman, Proc. Natl. Acad. Sci. U. S. A. **112**, 4952 (2015).
[32] R. Richert, Annu. Rev. Phys. Chem. **62**, 65 (2011).
[33] S. A. Mackowiak, L. M. Leone, and L. J. Kaufman, Phys. Chem. Chem. Phys. **13**, 1786 (2011).
[34] G. S. Harms, M. Sonnleitner, G. J. Schütz, H. J. Gruber, and T. Schmidt, Biophys. J. **77**, 2864 (1999).
[35] M. F. Gelin and D. S. Kosov, J. Chem. Phys. **125**, 054708 (2006).
[36] C.-Y. J. Wei, Y. H. Kim, R. K. Darst, P. J. Rossky, and D. A. Vanden Bout, Phys. Rev. Lett. **95**, 173001 (2005).
[37] S. A. Mackowiak, T. K. Herman, and L. J. Kaufman, J. Chem. Phys. **131**, 244513 (2009).
[38] J. Crocker and D. Grier, J. Colloid Interface Sci. **179**, 298 (1996).
[39] K. Stokely, A. S. Manz, and L. J. Kaufman, J. Chem. Phys. **142**, 114504 (2015).
[40] G. Hinze, G. Diezemann, and T. Basché, Phys. Rev. Lett. **93**, 203001 (2004).
[41] K. Paeng and L. J. Kaufman, Macromolecules **49**, 2876 (2016).
[42] C. M. Roland and R. Casalini, J. Chem. Phys. **119**, 1838 (2003).
[43] C. G. Robertson, P. G. Santangelo, and C. M. Roland, J. Non-Cryst. Solids **275**, 153 (2000).
[44] C. T. Thurau and M. D. Ediger, J. Chem. Phys. **116**, 9089 (2002).
[45] S. A. Mackowiak and L. J. Kaufman, J. Phys. Chem. Lett. **2**, 438 (2011).
[46] C. Y. J. Wei, C. Y. Lu, Y. H. Kim, and D. A. Vanden Bout, J. Fluoresc. **17**, 797 (2007).
[47] R. Böhmer, G. Hinze, G. Diezemann, B. Geil, and H. Sillescu, Europhys. Lett. **36**, 55 (1996).
[48] S. Léonard and L. Berthier, J. Phys.: Condens. Matter **17**, S3571 (2005).
[49] K. Kim and S. Saito, J. Chem. Phys. **138**, 12A506 (2013).
[50] M. T. Cicerone and M. D. Ediger, J. Chem. Phys. **103**, 5684 (1995).
[51] W. Kob, C. Donati, S. Plimpton, P. Poole, and S. Glotzer, Phys. Rev. Lett. **79**, 2827 (1997).
[52] P. G. Debenedetti and H. Stillinger Frank, Nature **410**, 259 (2001).
[53] A. Alegria, J. Colmenero, P. O. Mari, and I. A. Campbell, Phys. Rev. E **59**, 6888 (1999).